cis-Pt(NH_3)$_2$(GpG) Properties Interpreted through Comparison with Retro-Model GpG Adducts Having Carrier Ligands Designed to Slow Dynamic Motion and Control Cross-Link Handedness

Kevin M. Williams,[§] Leonardo Cerasino,[†] Giovanni Natile,*[,†] and Luigi G. Marzilli*[,§]

Contribution from the Department of Chemistry, Emory University, Atlanta, Georgia 30322, and Dipartimento Farmaco-Chimico, Università di Bari, via E. Orabona 4, 70125 Bari, Italy

Received December 8, 1999. Revised Manuscript Received May 22, 2000

Abstract: Cisplatin forms the *cis*-Pt(NH_3)$_2$(d(GpG)) intrastrand cross-link with DNA. Recently our experiments showed that the phosphodiester backbone can have a normal (1) or opposite (2) backbone propagation direction, leading to four conformer classes, HH1, HH2, ΔHT1, and ΛHT2, with the bases in either a head-to-head or head-to-tail orientation. In addition, since each G residue can be syn or anti and the base canting can be left (L) or right (R) handed, 32 variants of this cross-link are conceivable. Reported evidence supported the existence of only the two anti,anti HH1 variants, L in single strands and in *cis*-Pt(NH_3)$_2$(d(GpG)) and R in duplexes and in the ribo analogue, *cis*-Pt(NH_3)$_2$(GpG); in this regard, the latter is an excellent simple model of the DNA lesion. To test such interpretations, we used retro-model adducts (complexes with carrier ligands designed to slow dynamic motion in the d(GpG) cross-link). In retro-model d(GpG) adducts, anti,syn ΔHT1 L (5′-G anti and 3′-G syn) and anti,anti HH2 R variants have energy comparable to the previously known anti,anti HH1 variants; our work has led to the hypothesis that *cis*-Pt(NH_3)$_2$ adducts may actually be mixtures of conformers exchanging rapidly on the NMR time scale (Marzilli et al. *J. Am. Chem. Soc.* **1999**, *121*, 9133−9142). To test this hypothesis, we have now conducted NMR and CD spectroscopic studies of GpG adducts. Retro models containing the **Bip** (2, 2′-bipiperidine) carrier ligand in two enantiomeric forms, (*R*,*S*,*S*,*R*)-**Bip** and (*S*,*R*,*R*,*S*)-**Bip** (N, C, C, and N chelate ring atoms having the respective *R* or *S* configurations), control, respectively, the R and L base canting direction. For low pH (both G N1H's still protonated), (*R*,*S*,*S*,*R*)-**Bip**Pt(GpG) is almost entirely anti,anti HH1 R, but (*S*,*R*,*R*,*S*)-**Bip**Pt(GpG) is a mixture of anti,anti HH1 L and anti,syn ΔHT1 L forms, both *new* low pH forms for a GpG adduct. This HT variant grew to dominance after ∼3 d at pH ∼10 (both G N1's deprotonated). By pH jump experiments, we obtained NMR and deconvoluted CD spectra of both L variants of (*S*,*R*,*R*,*S*)-**Bip**Pt(GpG) at low and high pH. Spectral features of these L variants are present in *cis*-Pt(NH_3)$_2$(GpG) spectra, suggesting that the anti,anti HH1 R variant is not exclusively present but that ∼30% of other variants are present; N1H deprotonation alters the distribution of forms as found also for retro models. The results suggest that the spectroscopic and structural properties for retro models are directly relevant to cisplatin adducts.

Introduction

Cisplatin (*cis*-Pt(NH_3)$_2$$Cl_2$) displays exceptional anticancer activity against a variety of tumors; however, analogues of the type *cis*-Pt$X_2$$A_2$ [X_2 = anionic leaving ligand(s), A_2 = one diamine or two amine carrier ligands] are generally less active.[1−6] Despite the testing of over 3000 platinum compounds for anticancer activity, no drug with a different carrier ligand has gained wide clinical acceptance.[7] *cis*-Pt$X_2$$A_2$ compounds bind primarily to N7 of G residues (Figure 1). The most abundant adduct, a 1,2-intrastrand cross-link between adjacent G's, is thought to be responsible for the anticancer activity.[1−8] It is thus of some interest to understand how changes in the nonleaving carrier ligands influence the nature of the cross-linked adducts.[9]

NMR spectroscopy has been used extensively to characterize both small molecular models and oligonucleotide models of Pt-DNA adducts.[2] However, we have noted that interpretation of the NMR spectra is complicated by the "dynamic motion problem".[2,9,10] Briefly, when all nuclei of a given species are unique, multiple conformations in fast exchange on the NMR time scale cannot be distinguished from one dominant conformation; one set of resonances is expected for either case. Furthermore, for rapidly interchanging conformers, coupling constants and chemical shifts have values reflecting the weighted average for each conformer but NOE cross-peak intensities are biased toward the conformer with the shortest distance between

[§] Emory University.
[†] Università di Bari.

(1) Sherman, S. E.; Lippard, S. J. *Chem. Rev.* **1987**, *87*, 1153−1181.
(2) Ano, S. O.; Kuklenyik, Z.; Marzilli, L. G. In *Cisplatin: Chemistry and Biochemistry of a Leading Anticancer Drug*; Lippert, B., Ed.; Wiley-VCH: Weinheim, 1999; pp 247−291.
(3) Jamieson, E. R.; Lippard, S. J. *Chem. Rev.* **1999**, *99*, 2467−2498.
(4) Reedijk, J. *Chem. Commun.* **1996**, 801−806.
(5) Zamble, D. B.; Lippard, S. J. In *Cisplatin: Chemistry and Biochemistry of a Leading Anticancer Drug*; Lippert, B., Ed.; Wiley-VCH: Weinheim, 1999; pp 73−110.
(6) O'Dwyer, P. J.; Stevenson, J. P.; Johnson, S. W. In *Cisplatin: Chemistry and Biochemistry of a Leading Anticancer Drug*; Lippert, B., Ed.; Wiley-VCH: Weinheim, 1999; pp 31−69.
(7) Hambley, T. W. *Coord. Chem. Rev.* **1997**, *166*, 181−223.
(8) Dunham, S. U.; Lippard, S. J. *Biochemistry* **1997**, *36*, 11428−11436.
(9) Marzilli, L. G.; Ano, S. O.; Intini, F. P.; Natile, G. *J. Am. Chem. Soc.* **1999**, *121*, 9133−9142.
(10) Ano, S. O.; Intini, F. P.; Natile, G.; Marzilli, L. G. *J. Am. Chem. Soc.* **1998**, *120*, 12017−12022.

10.1021/ja994305t CCC: $19.00
Published on Web 08/08/2000

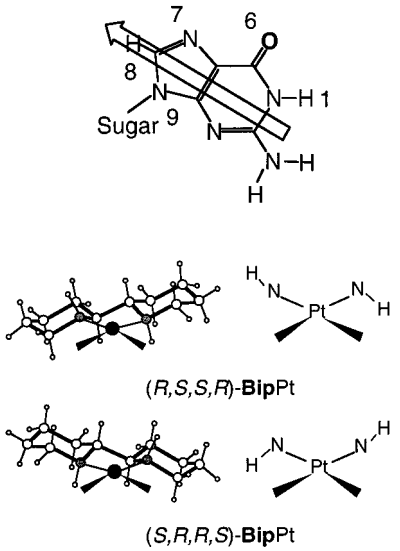

Figure 1. Top: Guanine base with partial numbering scheme and arrow notation indicating base orientation. Bottom: Ball and stick and shorthand notation for **Bip**Pt complexes. For clarity, the remaining coordination positions are not shown.

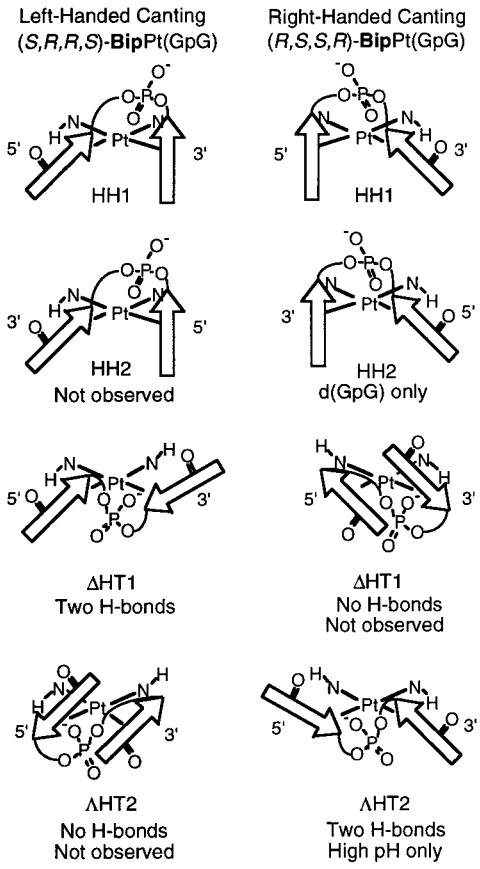

Figure 2. HH1, HH2, ΔHT1, and ΛHT2 conformers, showing variants with left-handed and right-handed canting.

nuclei. We illustrate the dynamic motion problem by comparing the *cis*-Pt$(NH_3)_2$(d(GpG)) and *cis*-Pt$(NH_3)_2$**G**$_2$ complexes (**G** = N9-substituted guanine derivative; the bold letter indicates a guanine not linked to another guanine). The cis guanine bases can have a head-to-head (HH) or a head-to-tail (HT) orientation (Figure 2). In *cis*-PtA_2**G**$_2$ adducts, there are two HT atropisomers, designated Δ and Λ, distinguishable by NMR spectroscopy only when the amine ligand(s) or the **G** ligands contain a chiral element. *cis*-Pt$(NH_3)_2$**G**$_2$ adducts, which show only one set of NMR resonances,[11,12] have been reasoned to exist as several conformers in fast chemical exchange.[12] This hypothesis is strongly supported by observations that bulky amine ligands can slow rotation of the **G** bases sufficiently to allow detection of different rotamers by NMR spectroscopy.[12−14] In contrast, it has been implied that *cis*-PtA_2(GpG) and *cis*-PtA_2(d(GpG)) cross-links exist essentially as only one conformer[15,16] and would have slow rotation around the Pt−N7 bond.[17] Both G residues of *cis*-Pt$(NH_3)_2$(d(GpG)) were assigned an anti conformation on the basis of T_1 relaxation times[18] and modeling;[19] the presence of two anti nucleotides led to the assignment of the HH1 conformation,[18−20] because all other conformers were suggested to have at least one syn base.[20] In all these studies, the backbone propagation direction is similar to that of B-DNA. A key NOE cross-peak connects the G H8's for the typical HH conformers.[2,16] In any case, HT conformers lack this peak because these forms have long H8−H8 distances.[2,9,10] Thus, a mixture of HH and HT conformers will still have this cross-peak and the HT form may go undetected.

Retro Models. Cisplatin is one of the simplest possible molecules. Elucidation of the properties of the adducts has been impeded by the simplicity and the dynamic nature of cisplatin adducts. In fact, since the features are very simple, many previous interpretations of these properties appear to be incorrect. In contrast to the simplification involved in most modeling of biological/medical systems, we are using a "retro-modeling" approach, wherein we introduce complexity into the carrier ligand both to make the spectral properties more informative and to diminish the dynamic motion.

Retro models with carrier ligands lacking C_2-symmetry lead to meaningful results.[21−25] However, our most informative retro-modeling efforts to detect and to characterize new cross-link forms employ specially designed C_2-symmetric ligands that are able to decrease fluxional motions by virtue of possessing rigid bulk along the coordination plane. Since these ligands lack significant bulk above and below the coordination plane, many conformations are possible for nucleic acid adducts. Furthermore, we have incorporated secondary amines near chiral carbons; these carbons restrict the amine configuration to a

(11) Dijt, F. J.; Canters, G. W.; den Hartog, J. H. J.; Marcelis, A. T. M.; Reedijk, J. *J. Am. Chem. Soc.* **1984**, *106*, 3644−3647.
(12) Cramer, R. E.; Dahlstrom, P. L. *J. Am. Chem. Soc.* **1979**, *101*, 3679−3681.
(13) Xu, Y.; Natile, G.; Intini, F. P.; Marzilli, L. G. *J. Am. Chem. Soc.* **1990**, *112*, 8177−8179.
(14) Kiser, D.; Intini, F. P.; Xu, Y. H.; Natile, G.; Marzilli, L. G. *Inorg. Chem.* **1994**, *33*, 4149−4158.
(15) Neumann, J.-M.; Tran-Dinh, S.; Girault, J.-P.; Chottard, J.-C.; Huynh-Dinh, T.; Igolen, J. *Eur. J. Biochem.* **1984**, *141*, 465−472.
(16) Bloemink, M. J.; Reedijk, J. *Cisplatin and Derived Anticancer Drugs: Mechanism and Current Status of DNA Binding*; Marcel Dekker: New York, 1996; Vol. 32.
(17) Berners-Price, S. J.; Ranford, J. D.; Sadler, P. J. *Inorg. Chem.* **1994**, *33*, 5842−5846.
(18) Girault, J.-P.; Chottard, G.; Lallemand, J.-Y.; Chottard, J.-C. *Biochemistry* **1982**, *21*, 1352−1356.
(19) den Hartog, J. H. J.; Altona, C.; Chottard, J.-C.; Girault, J.-P.; Lallemand, J.-Y.; de Leeuw, F. A. A. M.; Marcelis, A. T. M.; Reedijk, J. *Nucleic Acids Res.* **1982**, *10*, 4715−4730.
(20) Kozelka, J.; Fouchet, M.-H.; Chottard, J.-C. *Eur. J. Biochem.* **1992**, *205*, 895−906.
(21) Bloemink, M. J.; Perez, J. M. J.; Heetebrij, R. J.; Reedijk, J. *J. Biol. Inorg. Chem.* **1999**, *4*, 554−567.
(22) Wong, H. C.; Intini, F. P.; Natile, G.; Marzilli, L. G. *Inorg. Chem.* **1999**, *38*, 1006−1014.
(23) Wong, H. C.; Coogan, R.; Intini, F. P.; Natile, G.; Marzilli, L. G. *Inorg. Chem.* **1999**, *38*, 777−787.
(24) Inagaki, K.; Nakahara, H.; Alink, M.; Reedijk, J. *J. Chem. Soc., Dalton Trans.* **1991**, 1337−1341.
(25) Elizondo-Riojas, M.-A.; Bas, V.; Kozelka, J. *J. Biol. Inorg. Chem.* **2000**, *5*, 45−50.

particular chirality.[9,10,13,14,22,23,26−28] This design strategy has evolved to our recent use of 2,2′-bipiperidine (**Bip**);[9,10,28] the coordinated **Bip** ligand has two energetically favored C_2-symmetrical geometries, with *S,R,R,S* or *R,S,S,R* configurations at the asymmetric N, C, C, and N chelate ring atoms, Figure 1. The **Bip** ligand possesses in-plane bulk that greatly decreases the **G** rotation rate even in **Bip**Pt**G**$_2$ systems, allowing the chirality of the HT form to be determined.[28] Since carrier ligands such as **Bip** control which chirality (Δ or Λ, cf. Figure 2) of the HT conformers is preferred,[27] we call them chirality-controlling chelate (**CCC**) ligands. *Note that we denote diamine carrier ligands in boldface type.*

Two recent investigations[9,10] of **Bip**Pt(d(GpG)) adducts have demonstrated that the energy of other conformers of *cis*-PtA_2-(d(GpG)) adducts is in fact similar to that of the HH1 conformer. In the earlier study, (*R,S,S,R*)-**Bip**Pt(d(GpG)) was found to exist as two conformers with comparable stability.[10] The two adducts had similar ^{1}H and ^{31}P NMR spectra, $^3J_{H1'-H2'}$ and $^3J_{H1'-H2''}$ coupling constants, and NOE patterns. Each set of resonances belonged to an HH form with two anti G residues. These two distinct adducts differed, however, in the direction of propagation of the phosphodiester backbone with respect to the 5′-G; the new conformer is called HH2 (Figure 2). These adducts, which can be separated by HPLC, interconvert slowly when the solution is heated at 40 °C for several hours; interconversion is accomplished by rotation of both bases by ∼180° and concomitant adjustment of the phosphodiester backbone. Molecular mechanics and dynamics (MMD) calculations suggested that these two adducts should be similar in energy. The calculations indicated that the 3′-G would be canted in HH1 and the 5′-G would be canted in HH2 such that one amine-G O6 hydrogen bond could be formed in each conformer. These conformers are designated HH1 R and HH2 R to indicate that the canting is right-handed (Figure 2).

In the later study, two major conformers with similar populations were also found for (*S,R,R,S*)-**Bip**Pt(d(GpG)), the isomer of (*R,S,S,R*)-**Bip**Pt(d(GpG)) having the enantiomeric configuration of the **Bip** ligand.[9] One of these conformers, which had the NMR spectral features expected for an HH form, was determined to be HH1 L, with the 5′-G canted such that an amine-O6 hydrogen bond was possible (Figure 2). However, the other conformer, which had several unusual spectral characteristics (two upfield-shifted H8 signals and an upfield-shifted ^{31}P NMR signal at −4.6 ppm), was shown to be the anti,syn ΔHT1 conformer (Figure 2). This designation indicates that the HT bases have the Δ chirality, that the phosphodiester backbone propagation direction (relative to the 5′-G) is similar to that of the HH1 conformer, and that the 5′- and 3′-G's are anti and syn, respectively. These studies with the **Bip**Pt(d(GpG)) complexes established the following: (a) a different backbone propagation direction is possible; (b) HT forms are possible; and (c) an HT form can have a G residue with a syn conformation. Considering the four major conformer classes (HH1, HH2, ΔHT1, and ΛHT2) and the possible syn and anti conformation of each G nucleotide, 16 subconformers can be envisioned. In addition, each subconformer could be the R or L variant, leading to 32 possible variants. Indeed, in both **Bip**Pt-(d(GpG)) studies,[9,10] signals for minor conformers were detected, but at a level too low to provide structural information.

***cis*-Pt(NH$_3$)$_2$ Adducts.** Given the previous identification of only two of these 32 variants (anti,anti HH1 R and anti,anti HH1 L, except in one case of a hairpin[29]) for adducts with nonbulky carrier ligands and our recent results showing that other variants are possible for our adducts with specially designed carrier ligands, two reasonable alternative hypotheses emerge: First, the other variants are present in *cis*-Pt(NH$_3$)$_2$-(d(GpG)) but they have been missed because of the "dynamic motion problem". Alternatively, the special properties of the *cis*-Pt(NH$_3$)$_2$ moiety lead to a high or exclusive preference for the anti,anti HH1 R and L variants. If the latter hypothesis proves to be correct, adducts with other carrier ligands would have high populations of one or more of the other variants; as a consequence, these variants would have reduced activity (possibly because repair of these variants may be fast), explaining the difficulty of improving upon cisplatin and its very close analogues. Single-stranded N7−Pt−N7 cross-links generally have spectroscopic characteristics of an HH1 L variant.[18,20,30,31] In duplexes with the *cis*-Pt(NH$_3$)$_2$(d(GpG)) moiety, the HH1 R variant appears to dominate;[20] however, NMR spectra contain features consistent with a high fluxional character, which could be due to rapid equilibria involving other variants.[2] It is of some interest that no two NMR studies on duplexes have led to the same structures[2,32−35] and that none of the diverse solution structures has all the features recently found in the X-ray structure of a 16-mer bound to rat HMG1.[36] These variations in structure may be caused by spectral complications arising from dynamic motion centered at the cross-link.

d(GpG) vs (GpG) Adducts. Our work with **Bip**Pt(d(GpG))[9] has led us to question if *cis*-Pt(NH$_3$)$_2$(d(GpG)) is primarily anti,anti HH1 L as suggested in the literature.[20] In many respects, *cis*-Pt(NH$_3$)$_2$(GpG) is a better model than *cis*-Pt(NH$_3$)$_2$(d(GpG)) for the duplex DNA cross-link lesion since the dominant *cis*-Pt(NH$_3$)$_2$(GpG) conformer appears to be anti,anti HH1 R.[20] To test this interpretation and to further define the fundamental features of cross-linked adducts, we have now extended our approach to include **Bip**Pt(GpG) adducts. We have also characterized *cis*-Pt(NH$_3$)$_2$(GpG) by using ^{1}H and ^{31}P NMR spectroscopy and CD spectroscopy under our conditions to assess the literature suggestion that it is primarily anti,anti HH1 R and to compare the behavior of *cis*-Pt(NH$_3$)$_2$(GpG) with that of the less dynamic **Bip**Pt(GpG) adducts. Finally, we ask the question: Do GpG and d(GpG) adducts differ in retro models?

Materials and Methods

cis-Pt(NH$_3$)$_2$Cl$_2$ (Aldrich) and GpG (Et_3NH^+ salt, Sigma) were used as received. Syntheses of the (*S,R,R,S*)- and (*R,S,S,R*)-**Bip**Pt(NO$_3$)$_2$ complexes have been described.[10]

BipPt(GpG). (*S,R,R,S*)- or (*R,S,S,R*)-**Bip**Pt(NO$_3$)$_2$ (∼3 μmol) was added to D_2O (2.0 mL); after heating the solution gently to dissolve the solid, the pH (uncorrected) was adjusted to ∼2.5. GpG (∼3 μmol)

(26) Williams, K. M.; Cerasino, L.; Intini, F. P.; Natile, G.; Marzilli, L. G. *Inorg. Chem.* **1998**, *37*, 5260−5268.
(27) Marzilli, L. G.; Intini, F. P.; Kiser, D.; Wong, H. C.; Ano, S. O.; Marzilli, P. A.; Natile, G. *Inorg. Chem.* **1998**, *37*, 6898−6905.
(28) Ano, S. O.; Intini, F. P.; Natile, G.; Marzilli, L. G. *J. Am. Chem. Soc.* **1997**, *119*, 8570−8571.
(29) Iwamoto, M.; Mukundan, S., Jr.; Marzilli, L. G. *J. Am. Chem. Soc.* **1994**, *116*, 6238−6244.
(30) Fouts, C. S.; Marzilli, L. G.; Byrd, R. A.; Summers, M. F.; Zon, G.; Shinozuka, K. *Inorg. Chem.* **1988**, *27*, 366−376.
(31) den Hartog, J. H. J.; Altona, C.; van der Marel, G.; Reedijk, J. *Eur. J. Biochem.* **1985**, *147*, 371−379.
(32) Yang, D.; van Boom, S. S. G. E.; Reedijk, J.; van Boom, J. H.; Wang, A. H.-J. *Biochemistry* **1995**, *34*, 12912−12920.
(33) Herman, F.; Kozelka, J.; Stoven, V.; Guittet, E.; Girault, J.-P.; Huynh-Dinh, T.; Igolen, J.; Lallemand, J.-Y.; Chottard, J.-C. *Eur. J. Biochem.* **1990**, *194*, 119−133.
(34) Gelasco, A.; Lippard, S. J. *Biochemistry* **1998**, *37*, 9230−9239.
(35) Dunham, S. U.; Dunham, S. U.; Turner, C. J.; Lippard, S. J. *J. Am. Chem. Soc.* **1998**, *120*, 5395−5406.
(36) Ohndorf, U.-M.; Rould, M. A.; He, Q.; Pabo, C. O.; Lippard, S. J. *Nature* **1999**, *399*, 708−712.

in D_2O (1.5 mL) was added to the solution and the pH was adjusted to ~3.5. The sample was kept in an ice bath overnight. After checking an aliquot of the sample by NMR spectroscopy to confirm that the reaction was complete, the sample was transferred to an NMR tube and reduced in volume to ~500 μL by blowing air into the sample.

***cis*-Pt(NH$_3$)$_2$(GpG).** In a typical reaction, *cis*-Pt(NH$_3$)$_2$Cl$_2$ (2.7 μmol) was dissolved in D_2O (2.0 mL) at pH ~3 by brief heating and the solution was left overnight to ensure aquation. This solution was combined with a separate solution of GpG (~3 μmol) in D_2O (1.5 mL); after mixing, the pH was ~3.5. The reaction was monitored by ^{1}H NMR spectroscopy until no free GpG resonances were observed. The sample was reduced in volume to 500 μL.

NMR Spectroscopy. All NMR spectra were collected on a GE Omega GN-600 spectrometer. ^{1}H NMR spectra were collected using a spectral width of 6250 or 10000 Hz. The HOD peak was used as a secondary reference relative to 3-(trimethylsilyl)tetradeuteriosodium propionate (TSP). An exponential apodization function was used in processing spectra except when the line width was measured. ^{1}H-decoupled ^{31}P NMR spectra were recorded with a spectral width of 5000 Hz using trimethyl phosphate (TMP) in D_2O as an external reference.

2D NMR Spectroscopy. 2D NMR spectra (512 × 2048 matrices with a spectral window of 6250 or 10000 Hz in each dimension) were recorded at 5 °C. For the NOESY experiments, a 500 ms mixing time was used. A 1−2 s presaturation pulse was typically used to saturate the HOD resonance. Spectra were processed using Felix 97.0 (MSI) on a Silicon Graphics INDY R4400 workstation. Typical processing involved zero-filling the t_1 dimension to 2048 points, exponential multiplication (1.0 Hz line broadening) in t_2, and a sinebell function shifted 90° over all points in t_1.

CD Spectroscopy. CD spectra were acquired from 200 to 400 nm on a Jasco J-600 spectropolarimeter at room temperature in 0.1 M NaCl. Complex concentrations were 40−50 μM. Experience shows that with our instrument and these conditions, the most useful and reliable parts of the CD spectra are at longer wavelengths (>250 nm). CD spectra of (*S,R,R,S*)-**Bip**Pt(GpG) were collected at pH 3.5 and 10 before and after several days at high pH to obtain spectra for solutions containing different populations of the HH1 and ΔHT1 conformers. The actual population of each form was determined by integrating the H8 signals, or the H1′ signals when the H8 signals were partially exchanged with deuterium, in the analogous ^{1}H NMR spectrum. The CD spectra at a given pH are then represented by:

$$Ax + (1 - A)y = Q$$

$$Bx + (1 - B)y = R$$

where Q and R are the observed CD spectra, A and B are the decimal fractions of the HH form present, and x and y represent the deconvoluted HH and HT forms. Solving these equations yields the following:

$$y = (RA - BQ)/(A - B)$$

$$x = (Q/A) - ((1 - A)/A)y$$

Molecular Modeling. MMD calculations were performed on a Silicon Graphics INDY R5000 workstation using the InsightII package version 97.0 (MSI). A modified version of the AMBER force field[37] was employed. Charges and potential types were fixed using previously described methods.[37] Structures were minimized with 100 iterations of steepest descents minimization followed by a conjugate gradients minimization for 5000 iterations or until the Δ(rms) gradient was <0.001 kcal/(mol·Å). Dynamics were used to simulate heating to 300 K for 500 ps; 500 structures were generated and fully minimized. The solvent-exposed areas of individual atoms were measured by using InsightII to calculate a Connolly surface for each atom using a 1.4 Å probe radius. The total solvent-exposed area was taken as the sum of the contact and reentrant areas.[38]

(37) Yao, S. J.; Plastaras, J. P.; Marzilli, L. G. *Inorg. Chem.* **1994**, *33*, 6061−6077.

(38) Richards, F. M. *Annual Reviews in Biophysics and Bioengineering* **1977**, *6*, 151−176.

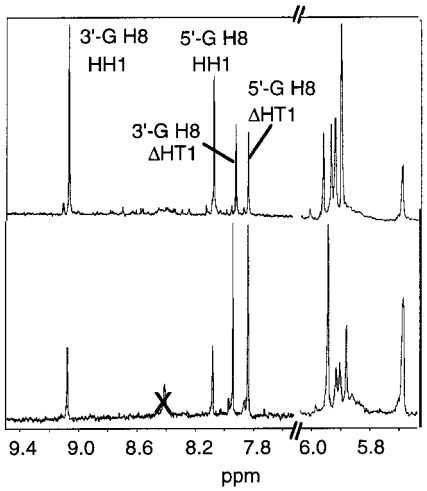

Figure 3. H8 and H1′ regions of the ^{1}H NMR spectrum of (*S,R,R,S*)-**Bip**Pt(GpG) at room temperature at pH 4 before (top) and immediately after (bottom) several days at pH 10. The **X** designates an impurity in this sample that is not observed in other (*S,R,R,S*)-**Bip**Pt(GpG) samples. Such erratic signals are often encountered and appear to be related to the source of D_2O, especially if the D_2O bottle was not freshly opened. (See ref 48 for an early example.)

Results

(*S,R,R,S*)-BipPt(GpG). When (*S,R,R,S*)-**Bip**Pt(NO$_3$)$_2$ was added to GpG at pH 3.5 and a ^{1}H NMR spectrum was collected 15 min later at 5 °C, two pairs of H8 signals were observed. The signals were sharp (2−4 Hz), consistent with either very fast or very slow exchange. The resonances of one pair are widely separated and exhibit a clear H8−H8 NOE cross-peak; both features indicate that the signals are from an HH form. This H8−H8 NOE cross-peak is relatively strong for a molecule of this type. This form was 80% abundant initially and 65% abundant after 1 day at room temperature; no further changes in intensity occurred with time, indicating that equilibrium had been reached (Figure 3). Thus, the HH form is favored by both kinetics and thermodynamics, and the exchange between forms is very slow. The NMR signals were assigned and the NOE data clearly show that both G residues of the HH form are anti (Supporting Information). The ^{1}H NMR H8 shifts of the HH form indicate that the 5′-G base must be canted; thus, the HH form could be either anti,anti HH1 L or anti,anti HH2 R (Figure 2).

In unrestrained MMD calculations, the anti,anti HH1 L and anti,anti HH2 L variants were calculated to be similar in energy (Table 2). No HH2 R variant was observed in the minimized structures generated from dynamics; when an anti,anti HH2 R variant was constructed and minimized, the resulting structure had only slight canting, and the energy was ~2 kcal/mol greater than that of the unrestrained HH1 L or HH2 L variants. Furthermore, the ^{1}H NMR H8 shifts are more similar to those of the anti,anti HH1 L variant of (*S,R,R,S*)-**Bip**Pt(d(GpG))[9] than those of the anti,anti HH2 R variant of (*R,S,S,R*)-**Bip**Pt(d(GpG)).[10] Thus, we conclude that the HH form of (*S,R,R,S*)-**Bip**Pt(GpG) is the anti,anti HH1 L variant. To our knowledge, *this is the first clear example of a left-handed anti,anti* HH1 *cis*-PtA$_2$(GpG) *variant.*

The other pair of H8 signals were both upfield; the lack of an H8−H8 cross-peak indicated that these signals belong to an HT form.[9] The value of 2.6 Hz for $^3J_{H1'-H2'}$ of the 3′-G sugar indicates that this sugar has either a mixture of N and S conformations or an unusual conformation. Unrestrained MMD calculations on the HH1, HH2, ΔHT1, and ΛHT2 conformers

Table 1. ^{1}H NMR Signals (ppm) for **Bip**Pt(d(GpG)), **Bip**Pt(GpG), and *cis*-Pt(NH$_3$)$_2$(GpG) Adducts[a]

adduct		G	H8	H1′	$J_{H1'-H2'}/J_{H1'-H2''}$	H2′	H2″	H3′	H4′
(*S*,*R*,*R*,*S*)-**Bip**Pt(d(GpG))[b]	HH1	5′	7.88	5.92	0/7.1	2.28	2.71	4.99	4.01
		3′	9.11	6.27	9.6/4.2	2.77	2.48	4.71	4.21
	ΔHT1	5′	7.77	6.17	0/5.4	2.72	2.58	3.90	
		3′	7.91	6.01	3.0/8.0	3.29	2.44	4.95	3.99
(*R*,*S*,*S*,*R*)-**Bip**Pt(d(GpG))[c]	HH 1	5′	8.76	6.32	0/6.8	2.48	2.73	4.82	4.13
		3′	8.22	6.23	9.5/4.9	2.32	2.37	4.54	4.16
	HH 2	5′	8.30	6.17	0/7.4	2.94	2.76	4.49	3.97
		3′	8.70	6.15	8.3/5.0	2.35	2.78	4.66	4.46
(*S*,*R*,*R*,*S*)-**Bip**Pt(GpG)	HH1	5′	8.10	5.86	0	4.22		4.90	4.25
		3′	9.10	5.90	8.3	4.72		4.47	4.32
	ΔHT1	5′	7.84	5.92	0	4.51		3.84	4.18
		3′	7.96	5.68	2.6	5.21		4.88	4.14
(*R*,*S*,*S*,*R*)-**Bip**Pt(GpG)	HH1	5′	8.78	6.09	0	4.23		4.70	4.39
		3′	8.10	5.88	7.7	4.24		4.30	4.27
cis-Pt(NH$_3$)$_2$(GpG)		5′	8.54	6.02	0	4.34		4.56	4.31
		3′	8.31	5.87	6.9	4.53		4.42	4.28
GpG		*d*	7.96	5.85	4.9				
		d	7.90	5.76	4.7				

[a] At pH 3.5 in D$_2$O at 5 °C. Coupling constants (Hz) measured at room temperature. [b] Reference 9. [c] Reference 10. [d] Did not distinguish 5′ or 3′; pH 6.5, room temperature.

Table 2. Selected Angles of Lowest Energy Structures from Unrestrained MMD Calculations for **Bip**Pt(GpG) Complexes and Comparison of Energies between Unrestrained and NMR-Restrained Structures

		χ (deg)		P (deg)[a]		energy (kcal/mol)	
Bip conf	variant	5′-G	3′-G	5′-G	3′-G	unrestrained	restrained
(*S*,*R*,*R*,*S*)	HH1 L	−162	6[b]	19	199	7.46	10.41
	HH2 L	10[b]	−158	23	39[c]	7.43	10.69
	ΔHT1 L	−154	68	31	39	6.01	6.01
	ΛHT2 R	16	−12	24	0	5.03	17.32
(*R*,*S*,*S*,*R*)	HH1 R	−170	−144	12	62[c]	8.13	8.75
	HH2 R	−67[b]	177	−11	168	5.74	11.39
	ΔHT1 L	−173	69	23	32	6.95	*d*
	ΛHT2 R	15	−14	−24	−1	4.72	*d*

[a] P = pseudorotation phase angle from the equation, tan $P = ((\nu_4 + \nu_1) - (\nu_3 + \nu_0))/(2\nu_2(\sin 36° + \sin 72°))$ (ν_{0-4} are the endocyclic sugar torsion angles). [b] These three angles are in the range to be considered syn; however, the H8−H2′ distance is less than the H8−H1′ distance. Furthermore, other low-energy structures have significantly different χ angles; thus, the values in this table should not be taken as evidence for a syn nucleotide. [c] In most other low-energy structures of these variants, the 3′-G sugars were *S*. [d] No restrained calculations were done for the HT forms of (*R*,*S*,*S*,*R*)-**Bip**Pt(GpG) because only an HH conformer was observed experimentally.

of (*S*,*R*,*R*,*S*)-**Bip**Pt(GpG) gave the lowest energy for the ΛHT2 conformer (Table 2); unrestrained calculations of certain *cis*-PtA$_2$(d(GpG)) complexes have also found HT conformers with lower energies than the HH conformers.[39] However, we have noted previously that calculated energy differences of only a few kilocalories/mole must be interpreted with caution and in conjunction with spectroscopic data.[9] The ΛHT2 model had both nucleotides syn, in contrast to experimental data for either of the observed forms; the energy-minimized structures of the ΛHT2 conformer had the R canting. The ΔHT1 model had only the 3′ nucleotide syn, in agreement with the experimental data observed for the HT form. Furthermore, the ^{1}H and ^{31}P NMR shifts of the HT form of (*S*,*R*,*R*,*S*)-**Bip**Pt(GpG) are very similar to those of the anti,syn ΔHT1 L variant of (*S*,*R*,*R*,*S*)-**Bip**Pt-(d(GpG)) (Tables 1 and 3);[9] therefore, we conclude that the HT form of (*S*,*R*,*R*,*S*)-**Bip**Pt(GpG) is the anti,syn ΔHT1 L variant. In support of the assignment of the HT form to ΔHT1 L, the ΔHT1 L model became >10 kcal/mol more stable than the ΛHT2 R model when NOE restraints for the HT form were included in the calculations (Table 2). *Thus, we have the first example of an HT cis-*PtA$_2$(GpG) *conformer.*

Table 3. pH Dependence of H8 and ^{31}P NMR Chemical Shifts (ppm)[a]

adduct	conformation		pH 3.5	pH 10
(*S*,*R*,*R*,*S*)-**Bip**Pt(GpG)	HH1	5′	8.07	7.41
		3′	9.08	9.10
		^{31}P	−3.17	−3.13
	ΔHT1	5′	7.83	7.56
		3′	7.93	7.73
		^{31}P	−4.78	−4.91
(*R*,*S*,*S*,*R*)-**Bip**Pt(GpG)	HH1	5′	8.81	8.73
		3′	8.08	7.68
		^{31}P	−3.32	−3.23
cis-Pt(NH$_3$)$_2$(GpG)		5′	8.51	7.97
		3′	8.28	8.16
		^{31}P	−3.64	−4.01

[a] In D$_2$O at room temperature. [b] This conformer was not observed at pH 4.

When the pH of a solution of (*S*,*R*,*R*,*S*)-**Bip**Pt(GpG) was raised to 10 and a spectrum was immediately recorded, several changes had occurred in the ^{1}H NMR spectrum (Table 3). The upfield 5′-G H8 signal of the HH1 conformer had shifted ∼0.65 ppm farther upfield, whereas the downfield 3′-G H8 signal had shifted almost insignificantly. Both H8 signals of the anti,syn ΔHT1 conformer had shifted upfield by ∼0.2 ppm. For both forms, the sugar resonances shifted little (typically 0.05 ppm or less) as the pH was raised to 10. The 3′-G $^3J_{H1'-H2'}$ coupling constant increased from 2.6 to 4.1 Hz as the pH was raised from 3 to 10, indicating an increase in S pucker of the 3′ sugar. The ^{31}P NMR signals of the HH1 and ΔHT1 conformers shifted slightly downfield and slightly upfield, respectively, when the pH was raised from 3 to 10 (Table 3).

In a spectrum of a sample of (*S*,*R*,*R*,*S*)-**Bip**Pt(GpG) kept at high pH (∼10) for 1 day, the intensities of the H1′ signals of the ΔHT1 and HH1 conformers were approximately equal. After 6 days, the signals of the ΔHT1 conformer comprised 70% of the NMR intensity, indicating that the anti,syn ΔHT1 conformer is favored at high pH. At pH ∼10, the 3′-G H8 signal of each conformer decreased with time. Thus, 3′-G H8 had a faster exchange rate with D$_2$O than 5′-G H8, consistent with a report on *cis*-Pt(NH$_3$)$_2$(GpG).[18] From a comparison of H8 to H1′ signal intensities, the half-life of the exchange of the 3′-G H8 proton of the HH1 conformer of (*S*,*R*,*R*,*S*)-**Bip**Pt(GpG) was estimated to be ∼2 days. The 3′-G H8 proton of the ΔHT1 conformer

(39) Hambley, T. W.; Ling, E. C. H.; Messerle, B. A. *Inorg. Chem.* **1996**, *35*, 4663−4668.

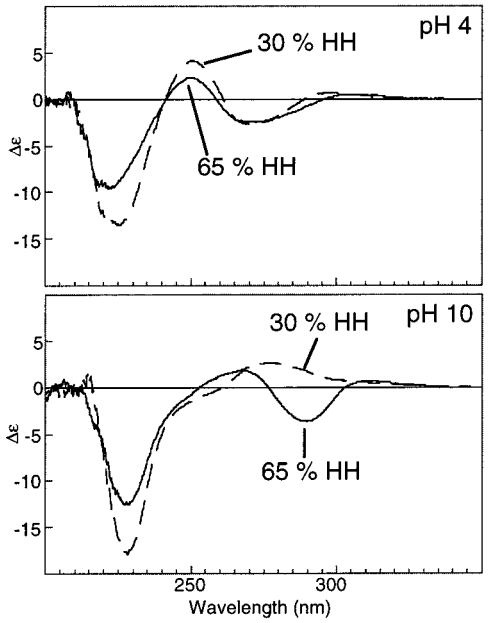

Figure 4. CD spectra of (*S,R,R,S*)-**Bip**Pt(GpG) at room temperature at pH 4 (top) and 10 (bottom) with 65% HH (solid line) and 30% HH (dashed line).

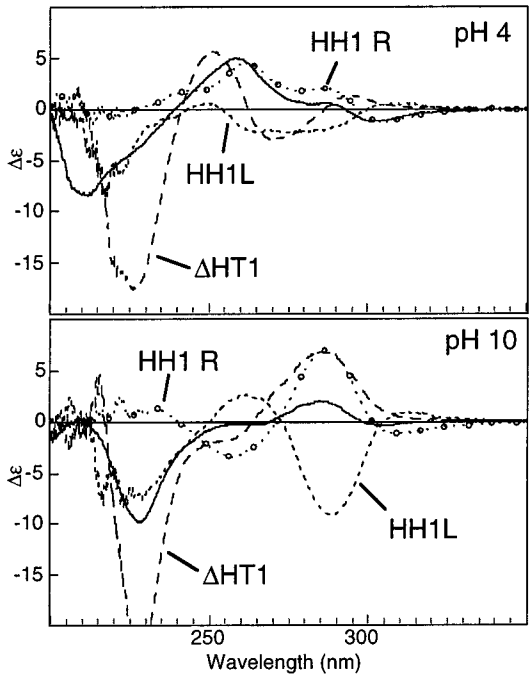

Figure 5. Room-temperature CD spectra at pH 4 (top) and 10 (bottom) of *cis*-Pt(NH_3)$_2$(GpG) (solid line) superimposed with deconvoluted spectra of the ΔHT1 (dashed line) and HH1 (dotted line) conformers of (*S,R,R,S*)-**Bip**Pt(GpG) and with (*R,S,S,R*)-**Bip**Pt(GpG) (dotted line with circles).

exchanged with deuterium more slowly than did that of the HH1 conformer; the rate of deuterium exchange for the H8 protons of the ΔHT1 conformer could not be estimated because of interconversion between the HH1 and ΔHT1 conformers.

In spectra recorded 20 min after the pH of the high pH sample of (*S,R,R,S*)-**Bip**Pt(GpG) was lowered to 4.4, the ΔHT1 conformer remained 70% abundant, indicating that the HH1 to ΔHT1 conversion is slow at room temperature (Figure 3). After ∼5 days at low pH, the HH1:ΔHT1 ratio had returned to 65:35, its value before the pH was raised. No immediate change in the spectrum was observed when the sample was heated to 65 °C at low pH. However, when the sample was kept at 65 °C overnight, the HH1:ΔHT1 ratio became ∼1:1, demonstrating that the HH1 conformer is less favored at 65 °C. The HH1:ΔHT1 ratio returned to its initial value of 65:35 after several days at room temperature.

The CD spectrum of (*S,R,R,S*)-**Bip**Pt(GpG) was recorded at pH 4 in 0.1 M NaCl at room temperature (Figure 4). The pH of the sample was then raised to 10 and a CD spectrum was acquired immediately. We call this a pH jump experiment. Because the NMR studies demonstrated that the HH1 to ΔHT1 equilibration is very slow, the immediate changes observed must be due to N1H deprotonation. The CD spectrum at pH 10 slowly changed over several days as the population of the ΔHT1 conformer increased. After ∼3 days at pH 10, the changes ceased, indicating that equilibrium had been reached. The pH was then dropped to 4 and a CD spectrum acquired immediately; this spectrum differed from the original pH 4 spectrum (Figure 4). After several days, the spectrum had reverted to its original form, indicating that the changes were reversible. Knowing the HH1:ΔHT1 equilibrium ratios from our ^{1}H NMR spectra, we were able to obtain deconvoluted CD spectra of the HH1 and ΔHT1 conformers at pH 4 and 10 (Figure 5).

***(R,S,S,R)*-BipPt(GpG).** At pH 4.4, the NMR spectrum of (*R,S,S,R*)-**Bip**Pt(GpG) showed only two sharp H8 signals (Figure 6). These H8 signals were well separated and connected by an NOE cross-peak, indicating that they arise from an HH form. The presence of only one form differs from the case of (*R,S,S,R*)-**Bip**Pt(d(GpG)), which had two forms.[10] When the pH of the (*R,S,S,R*)-**Bip**Pt(GpG) sample was raised to 10.0 and a spectrum

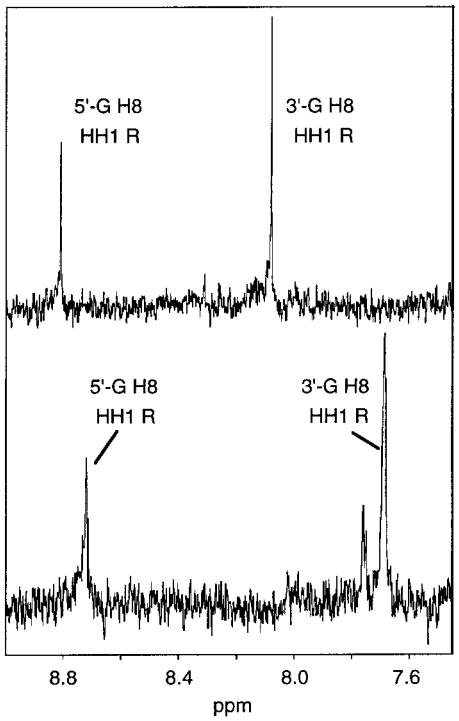

Figure 6. H8 region of the ^{1}H NMR spectrum of (*R,S,S,R*)-**Bip**Pt-(GpG) at pH 4.4 (top) and at pH 9.8 after 3 days (bottom) in D_2O at room temperature. The small peaks at ∼7.75 ppm are thought to be due to the ΛHT2 conformer.

recorded immediately, the 5′-G H8 and 3′-G H8 signals had shifted upfield (Table 3). The sugar resonances shifted very little (less than 0.05 ppm) as the pH was raised to 10. Only a small downfield shift was observed in the ^{31}P NMR signal when the pH was raised. After the high pH sample was left for 1 day, two small ^{1}H NMR signals at 7.76 and 7.75 ppm had emerged (Figure 6); these signals did not grow in intensity over the next

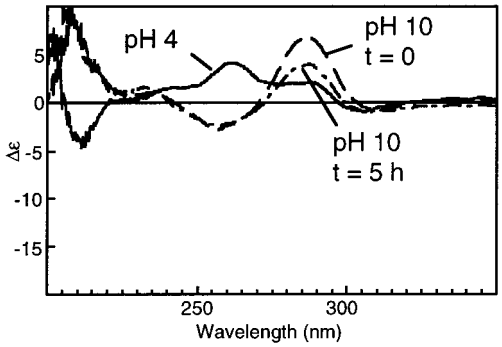

Figure 7. CD spectra of (*R,S,S,R*)-**Bip**Pt(GpG) at pH 4 (solid line) and at pH 10 at $t = 0$ (dashed line) and 5 h (dotted line).

2 days at pH 9.8. The signals could be due to an HT form that becomes more favored at high pH or to partial isomerization of the **Bip** ligand. When the pH was lowered to 3 and a spectrum was recorded immediately, the new signals had disappeared, indicating that this form is very unstable at pH 3, where N1 would be protonated. Because the new form disappeared, it cannot be due to isomerization of the **Bip** ligand. For the HH conformer, the 5′-G H8 signal exchanged with deuterium faster than the 3′-G H8 signal at pH ∼10.

Unrestrained MMD calculations of the HH1, HH2, ΔHT1, and ΛHT2 conformers of (*R,S,S,R*)-**Bip**Pt(GpG) were performed (Table 2). The ΔHT1 and ΛHT2 conformers had one or both nucleotides syn, respectively, in contrast to experimental data on the observed form indicating both are anti (Supporting Information); furthermore, the HT conformers would not be expected to show an H8−H8 NOE cross-peak. Because the 5′-G H8 signal is downfield of the 3′-G H8 signal, the 3′ base must be canted in the observed form; therefore, the observed form must be HH1 R or HH2 L. The HH1 and HH2 conformers obtained from unrestrained MMD calculations were both the R variant. The HH2 R conformer was initially calculated to be more stable than the HH1 R variant; however, when restraints based on 300 ms NOESY data were included in the calculations, the HH2 conformer became >2.5 kcal/mol less stable than the HH1 conformer (Table 2). Even in the restrained calculations the HH2 conformer was the R variant, but this variant is inconsistent with the H8 shifts. Thus, we conclude that the experimentally observed HH form must be anti,anti HH1 R.

The CD spectrum of (*R,S,S,R*)-**Bip**Pt(GpG) at pH 4 (Figure 7) has weaker features than those found in spectra of HT forms. This pH 4 spectrum of an HH1 R form is more similar in shape to those found for HH forms; the shape can be compared to that of an HH1 L variant, e.g. the spectrum of opposite sign observed for the HH1 L variant of (*S,R,R,S*)-**Bip**Pt(GpG) (Figure 5). The pH was jumped to 10 and a spectrum was acquired immediately (Figure 7). When the pH was kept at 10 for several hours, the feature at ∼290 nm decreased in intensity (Figure 7); after ∼5 h no further significant changes occurred. An increase at ∼290 nm would have been observed if the new ^{1}H NMR signals were due to the ΔHT1 variant; the observed decrease suggests that the new form is a ΛHT2 conformer. However, because only a small population of this form is present, we were unable to characterize it further. The pH was dropped to 4, and the spectrum recorded immediately was nearly identical with the original pH 4 spectrum.

***cis*-Pt(NH$_3$)$_2$(GpG).** At 21 °C and pH 3.5, the downfield H8 signal (8.51 ppm) of *cis*-Pt(NH$_3$)$_2$(GpG) had a line width of ∼10 Hz, whereas the line width of the upfield H8 signal (8.28 ppm) was ∼4 Hz. When the temperature was lowered to 5 °C, these signals broadened to 20 and 5 Hz, respectively. Because N7−Pt−N7 cross-links have been found to have an N conformation for the 5′ sugar in solution,[2,9,10,19] crystal structures,[36,40] and structures generated by MMD calculations,[2,9,10,41] the singlet at 6.02 ppm was assigned to 5′-G H1′, and the doublet at 5.87 ppm was assigned to 3′-G H1′. This is the starting point for the following complete assignment of the ^{1}H NMR signals from the NOESY and COSY spectra (Table 1); to our knowledge, this is the first reported 2D NMR-based assignment of the signals of *cis*-Pt(NH$_3$)$_2$(GpG) (Supporting Information). Our assignments of the 5′-G H8 and 3′-G H8 signals agree with previous assignments based on deuterium exchange.[18] Furthermore, NOE cross-peaks suggest that the nucleotides are primarily anti (Supporting Information), also in agreement with the literature.

As the pH of a sample of *cis*-Pt(NH$_3$)$_2$(GpG) in D$_2$O was raised above ∼7, the H8 signals began to shift upfield (Table 3); by pH 10, the 5′-G H8 resonance had shifted upfield of the 3′-G H8 resonance, consistent with a previous study.[18] At pH 10 and 5 °C, the line widths of the 5′-G and 3′-G H8 signals were ∼12 and ∼18 Hz, respectively; thus, the 3′-G H8 signal had broadened, whereas the 5′-G H8 signal had sharpened as the pH was raised from 4 to 10. To determine if a conformational change had occurred, a NOESY spectrum was recorded at pH 9.9 and the signals were assigned (Supporting Information). The 3′-G H8 signal had a weak H8−H1′ NOE cross-peak and a stronger H8−H2′ NOE cross-peak (Supporting Information), suggesting that this nucleotide still has primarily an anti conformation. However, since no 5′-G H8−H1′ NOE cross-peak was seen, observation of the 3′-G H8−H1′ NOE cross-peak suggests that the 3′-G has more syn character than the 5′-G or that there are multiple forms, some with a syn 3′-G and some with an anti 3′-G.

Because the ^{31}P NMR shifts of the HH and ΔHT conformers of the **Bip**Pt(GpG) adducts differ considerably, we collected the ^{31}P NMR spectrum of *cis*-Pt(NH$_3$)$_2$(GpG) at low and high pH. At pH 3.5, the shift of the one ^{31}P NMR signal observed at −3.64 ppm at room temperature is between the values observed for the HH1 conformers of **Bip**Pt(GpG) and the ΔHT1 conformer of (*S,R,R,S*)-**Bip**Pt(GpG) (Table 3), suggesting that a small population of the ΔHT1 conformer may be present in *cis*-Pt(NH$_3$)$_2$(GpG). As the pH of a sample of *cis*-Pt(NH$_3$)$_2$(GpG) was raised to 10, the ^{31}P NMR signal shifted even farther upfield, to −4.01 ppm; in contrast, the ^{31}P NMR signals of the **Bip**Pt(GpG) adducts were not significantly affected by pH (Table 3). These shifts suggest that the HT population increases upon N1H deprotonation at high pH, as observed for (*S,R,R,S*)-**Bip**Pt(GpG).

The CD spectrum of *cis*-Pt(NH$_3$)$_2$(GpG) was collected at pH 4 (Figure 5). The pH was jumped to 10 and a spectrum was acquired within 20 s (Figure 5); no further changes occurred over time, indicating that any conformational change that results from a change in pH must be very fast. When the pH was lowered to 4, the spectrum immediately reverted to its original pH 4 shape. The spectra we collected are similar to those observed previously.[42]

Discussion

Features of the **Bip**Pt(GpG) complexes have many similarities to those of the **Bip**Pt(d(GpG)) complexes, the first N7−Pt−N7

(40) Sherman, S. E.; Gibson, D.; Wang, A. H.-J.; Lippard, S. J. *Science (Washington, D.C.)* **1985**, *230*, 412−417.
(41) Kozelka, J.; Archer, S.; Petsko, G. A.; Lippard, S. J. *Biopolymers* **1987**, *26*, 1245−1271.
(42) Chottard, J.-C.; Girault, J.-P.; Chottard, G.; Lallemand, J.-Y.; Mansuy, D. *J. Am. Chem. Soc.* **1980**, *102*, 5565−5572.

cross-linked adducts for which the existence of multiple non-HH1 conformations of the d(GpG) moiety was demonstrated.[9,10] As mentioned in the Introduction, for *both* the (*S*,*R*,*R*,*S*)- and (*R*,*S*,*S*,*R*)-**Bip**Pt(d(GpG)) isomers, *two* forms were found to dominate. In the *S*,*R*,*R*,*S* case the forms are both left-handed but in the *R*,*S*,*S*,*R* case they are both right-handed. For this and other reasons, we call such chiral C_2-symmetric carrier ligands chirality-controlling chelate ligands (**CCC**).[2,27] However, since the wagging motion relating a right-handed and left-handed form, e.g. HH1 R and HH1 L, is fast (see below), we cannot exclude small populations of the less favored handedness for a particular conformer. Thus, we will frequently be cautious and state that a variant is almost exclusively the R variant. However, the interconversion between conformers from different classes, e.g. HH1 and ΔHT1, is normally slow for retro models.

For (*S*,*R*,*R*,*S*)-**Bip**Pt(d(GpG)), one HH form and one HT form were observed to dominate at equilibrium.[9] These two forms were determined to be anti,anti HH1 L and anti,syn ΔHT1 L on the basis of experimental observations and restrained MMD calculations. The ^{1}H and ^{31}P NMR spectra of (*S*,*R*,*R*,*S*)-**Bip**Pt-(GpG) have features very similar to those of (*S*,*R*,*R*,*S*)-**Bip**Pt-(d(GpG)) (Tables 1 and 3), strongly suggesting that the *two* dominant forms observed for (*S*,*R*,*R*,*S*)-**Bip**Pt(GpG) are the anti,anti HH1 L and anti,syn ΔHT1 L variants. The very similar CD spectra observed for (*S*,*R*,*R*,*S*)-**Bip**Pt(GpG) (Figure 4) and (*S*,*R*,*R*,*S*)-**Bip**Pt(d(GpG)) support this NMR-based conclusion.[43] Both (*S*,*R*,*R*,*S*)-**Bip**Pt(d(GpG)) and (*S*,*R*,*R*,*S*)-**Bip**Pt(GpG) have ∼65% of the HH1 L variant at pH 4 at equilibrium; however, in early stages of the reaction, (*S*,*R*,*R*,*S*)-**Bip**Pt(GpG) has ∼80% HH1 L and 20% ΔHT1 variants, whereas (*S*,*R*,*R*,*S*)-**Bip**Pt-(d(GpG)) has approximately equal populations of HH1 L, ΔHT1, and a thermodynamically unfavorable third variant which over time preferentially forms the anti,syn ΔHT1 variant.[9] Thus, the 2′-OH groups in GpG appear to influence the kinetic pathway but not the equilibrium position or the conformation of adducts when the carrier ligand is (*S*,*R*,*R*,*S*)-**Bip**.

For (*R*,*S*,*S*,*R*)-**Bip**Pt(d(GpG)), we reported that the two conformers were both HH (HH1 R and HH2 R) with ^{1}H NMR spectra having a similar appearance, including two well-dispersed H8 signals (Table 1).[10] However, assignment via 2D NMR indicated an important difference: the HH1 conformer has an upfield 3′-G H8 signal, while the HH2 conformer has an upfield 5′-G H8 signal. In contrast, there is only *one* dominant form for (*R*,*S*,*S*,*R*)-**Bip**Pt(GpG); this is an HH form. The ^{1}H NMR signals of the HH form are in complete accord with the anti,anti HH1 R variant (Figure 2). On the other hand, the anti,anti HH2 R variant is ∼2.5 kcal/mol less stable than the anti,anti HH1 R variant in restrained MMD calculations (Table 2), and the HH2 R variant would not give the observed H8 shift pattern (Figure 2). Thus, we conclude that the one (*R*,*S*,*S*,*R*)-**Bip**Pt(GpG) form observed below pH 7.5 clearly is primarily the HH1 R variant.

For all of the **Bip**Pt(d(GpG))[43] and **Bip**Pt(GpG) variants, downfield H8 signals shift very little with increasing pH, while upfield H8 signals shift farther upfield (Table 3). A base with an upfield-shifted H8 signal is typically canted; the cause of the canting could be the formation of an amine-O6 hydrogen bond (Figure 2). Upon N1H deprotonation, this hydrogen bond would be expected to be stronger because of increased electron density at G O6 (Figure 1); a stronger hydrogen bond could cause a greater canting, which would explain the greater upfield shift. However, an alternative explanation for the upfield shift at high pH is that increased electron density in a deprotonated base leads to a greater shielding effect. Regardless of its specific cause, the upfield change in H8 shift is indicative of a canted guanine base.

The 3′-G H8 proton of both (*S*,*R*,*R*,*S*)-**Bip**Pt(GpG) conformers exchanged with D_2O more rapidly than the 5′-G H8 proton, in agreement with previous observations for *cis*-Pt$(NH_3)_2$(GpG), *cis*-Pt$(NH_3)_2$(d(GpG)), and *cis*-Pt$(NH_3)_2$(d(pGpG)).[18] However, the 5′-G H8 exchanged more rapidly than the 3′-G H8 in the (*R*,*S*,*S*,*R*)-**Bip**Pt(GpG) complex. The more rapidly exchanging proton in each complex gives the more downfield signal at high pH. This observation suggests that the H8 proton of a canted base may be less accessible to attack by OD^-, decreasing the rate of D_2O-H8 exchange.

For (*S*,*R*,*R*,*S*)-**Bip**Pt(GpG), the anti,anti ΔHT1 L variant becomes favored at high pH (Figure 3). We were able to obtain deconvoluted CD spectra of the anti,anti HH1 L and anti,syn ΔHT1 L variants (Figure 5). Previously it was suggested that the signs of the CD spectra of *cis*-PtA_2**G**$_2$ complexes were indicative of handedness of an HT conformer;[44,45] however, more recent evidence suggests that the CD spectra are more indicative of the Δ vs Λ population of the HT rotamers.[27] The anti,anti HH1 conformers of (*S*,*R*,*R*,*S*)-**Bip**Pt(GpG) (L variant) and (*R*,*S*,*S*,*R*)-**Bip**Pt(GpG) (R variant) have CD spectra that are similar in shape but opposite in sign both at pH 4 (>250 nm only) and at pH 10 (Figure 5). This result suggests that the handedness of the base canting influences the CD spectra of HH conformers, or at least of the HH1 conformers. However, the HH1 L and ΔHT1 L conformers both have the L canting but the spectra are very different; thus, the relative HH vs HT orientation of the bases has a major effect on the CD spectrum. The CD spectra of the HH1 L and HH1 R variants are weaker in intensity than that of the ΔHT1 L variant (Figure 5), in support of recent observations that the CD spectra of *cis*-PtA_2**G**$_2$ complexes are reflective of the dominant HT conformers.[27,46]

Although (*R*,*S*,*S*,*R*)-**Bip**Pt(GpG) exists as an anti,anti HH1 conformer in essentially exclusively the R variant at low pH, additional ^{1}H NMR signals corresponding to a new form emerge slowly at pH 10 (Figure 6). Since the process is slow, the new form probably is from a different conformer class. The upfield position of the new signals suggests that it is an HT form since all known HH forms have at least one downfield H8 signal. However, we cannot characterize the form by 2D NMR methods because it is a minor form and H8 exchange occurs at this pH. However, its formation is reversible and the upfield shifts indicate that both bases are canted. High pH favors HT forms as well as G O6 H-bonding since N1H deprotonation makes G O6 a better hydrogen-bonding group. A ΔHT1 L conformer would be disfavored by clashes between G O6 and the methylene groups of the **Bip** ligand, but a ΛHT2 R conformer could form two G O6 to **Bip** NH H-bonds in an (*R*,*S*,*S*,*R*)-**Bip** complex (Figure 2). Thus, it seems likely the new form is a ΛHT2 conformer. These considerations are supported by CD evidence. The CD spectrum of the ΔHT1 conformer of (*S*,*R*,*R*,*S*)-**Bip**Pt(GpG) (Figure 5) has features similar to those of *cis*-PtA_2**G**$_2$ complexes that favor the ΔHT conformer.[22,26,27] Thus, the linking of the G's by a backbone seems to have no major effect on the CD spectrum. Since *cis*-PtA_2**G**$_2$ complexes that favor the ΔHT and the ΛHT conformer have CD spectra

(43) Williams, K. M.; Cerasino, L.; Natile, G.; Marzilli, L. G. Manuscript in preparation.

(44) Pasini, A.; Giacomo, L. D. *Inorg. Chim. Acta* **1996**, *225*−*230*, 225−230.

(45) Gullotti, M.; Pacchioni, G.; Pasini, A.; Ugo, R. *Inorg. Chem.* **1982**, *21*, 2006−2014.

(46) Ano, S. O.; Intini, F. P.; Natile, G.; Marzilli, L. G. *Inorg. Chem.* **1999**, *38*, 2989−2999.

with opposite sign,[23,26,27] the CD spectrum of a ΛHT2 conformer should be opposite in sign to that of a ΔHT1 conformer. The changes with time in the CD spectrum of (*R,S,S,R*)-**Bip**Pt(GpG) at high pH corresponding to the build-up of the HT form (Figure 7) were opposite to what would be expected if the new species were a ΔHT1 conformer; thus, the new HT form is almost undoubtedly a ΛHT2 conformer. This is the first evidence for a ΛHT2 conformer; *the* **Bip**Pt *retro models have thus provided evidence for all three previously missing classes* (ΛHT2, ΔHT1, and HH2) of the *four* conformer classes.

It is quite interesting that the anti,anti HH2 R variant is not detected for (*R,S,S,R*)-**Bip**Pt(GpG) since it is quite abundant for (*R,S,S,R*)-**Bip**Pt(d(GpG)). This result is even more intriguing since the three observed abundant **Bip**Pt(GpG) variants (HH1 L, HH1 R, and ΔHT1) have ^{1}H and ^{31}P NMR and CD spectra very similar to those of the three corresponding **Bip**Pt(d(GpG)) variants.[9,10,43] This finding indicates that in the observed variants, the GpG and the d(GpG) moieties have very similar structures. To explain these similarities and differences, we used MMD calculations and focused on the ribose 2′-hydroxyl groups of GpG.

The lowest-energy structures for (*R,S,S,R*)-**Bip**Pt(GpG) obtained from both unrestrained and NMR-restrained MMD calculations predicted a hydrogen bond between the 5′-G 2′-OH and a phosphate oxygen (O···O distance, 2.77 Å) in the anti,anti HH1 R variant and a hydrogen bond between the 3′-G 2′-OH and 3′-G N3 atoms (N···O distance, 2.84 Å) in the anti,anti HH2 R variant (Supporting Information). However, when we compare the solvent-exposed areas (Supporting Information), we find that such H-bonding is more likely to be a net stabilizing effect in the observed anti,anti HH1 R variant. Thus, this hydrogen bonding may displace the HH1 R to HH2 R equilibrium toward HH1 R to such an extent that the HH2 R variant is not detected. No such stabilizing effect is possible in the d(GpG) adduct consistent with the similar stability of the anti,anti HH2 R and anti,anti HH1 R variants of (*R,S,S,R*)-**Bip**Pt-(d(GpG)).

Our modeling shows no hydrogen bonding involving the 2′-OH in any anti,syn ΔHT1 structures nor in any lowest-energy structures of the anti,anti HH1 L variant of (*S,R,R,S*)-**Bip**Pt-(GpG). If such hydrogen bonding were present in solution for the HH1 L conformer, this conformer would be more favorable in (*S,R,R,S*)-**Bip**Pt(GpG) than in (*S,R,R,S*)-**Bip**Pt(d(GpG)). However, we see the same equilibrium HH:HT ratios for (*S,R,R,S*)-**Bip**Pt(GpG) and (*S,R,R,S*)-**Bip**Pt(d(GpG)). We conclude that the HH1 L variant of (*S,R,R,S*)-**Bip**Pt(GpG) does *not* form a 5′-G 2′-OH-phosphate group hydrogen bond in solution. These modeling results support pioneering modeling results on *cis*-Pt(NH$_3$)$_2$(GpG) (see below).

Against this background of a substantial body of modeling NMR and CD data for several unique conformers of the **Bip**Pt-(GpG) adducts, we now turn to consider the *cis*-Pt(NH$_3$)$_2$(GpG) properties, especially as these relate to our hypothesis that *cis*-Pt(NH$_3$)$_2$(GpG) is a dynamic mixture of conformers from different classes. To summarize previous work, NMR and CD spectroscopy as well as modeling led to the conclusion that *cis*-Pt(NH$_3$)$_2$(GpG) exists almost exclusively as the anti,anti HH1 conformer.[18,20,42] The H8 shifts were interpreted to indicate R base canting for *cis*-Pt(NH$_3$)$_2$(GpG) (and L base canting for Pt(NH$_3$)$_2$(d(GpG))).[20] For our **Bip**Pt(GpG) adducts, the dynamic motion is decreased and the canting is controlled by the carrier ligand; thus, we have the advantage that we can obtain information on the R and L variants separately. Also, we have assigned the H2′, H3′, and H4′ NMR signals of *cis*-Pt(NH$_3$)$_2$-(GpG). When we employed the same conditions, our ^{1}H NMR and CD spectral results for *cis*-Pt(NH$_3$)$_2$(GpG) are similar to those reported previously.[18] With this more complete information, we can now reassess the behavior of *cis*-Pt(NH$_3$)$_2$(GpG), first at low and then at high pH. Finally, we shall consider the modeling results reported for *cis*-Pt(NH$_3$)$_2$(GpG).

For low pH, the ^{1}H NMR chemical shifts of *cis*-Pt(NH$_3$)$_2$-(GpG) are most similar to those of the (*R,S,S,R*)-**Bip**Pt(GpG) anti,anti HH1 conformer (Table 1), which exists essentially only as the R variant. Furthermore, the CD spectrum of *cis*-Pt(NH$_3$)$_2$-(GpG) in the 250−350 nm region is similar to that of (*R,S,S,R*)-**Bip**Pt(GpG) (Figure 5). Thus, our data appear to support the previous conclusion that *cis*-Pt(NH$_3$)$_2$(GpG) exists primarily as the anti,anti HH1 R variant at low pH (Figure 2).[20]

Despite these points of agreement with previous work, some important differences in shifts between *cis*-Pt(NH$_3$)$_2$(GpG) and (*R,S,S,R*)-**Bip**Pt(GpG) suggest that the former has nonnegligible populations of variants in addition to the anti,anti HH1 R variant. For example, a small population of the anti,syn ΔHT1 L variant would account for the slightly more upfield than normal shift of the *cis*-Pt(NH$_3$)$_2$(GpG) ^{31}P NMR signal (Table 3). Furthermore, exchange between the anti,anti HH1 R and anti,syn ΔHT1 L variants would explain the broadness observed for the more downfield of the two *cis*-Pt(NH$_3$)$_2$(GpG) H8 signals; because both H8 signals of the anti,syn ΔHT1 L variant are normally relatively upfield, anti,anti HH1 R to anti,syn ΔHT1 L exchange would cause the more downfield 5′-G H8 signal to be broader than the relatively upfield 3′-G H8 signal. The energy barrier for wagging between the anti,anti HH1 R and L variants was estimated by using MMD calculations. We energy-minimized structures of these variants and found that these were comparable in energy (<1 kcal/mol difference). We then rotated both bases by 5° increments, converting the L into the R variant. At each increment the structure was minimized. None of these structures had energies >1 kcal/mol higher than that of either of the two end structures, suggesting little barrier to wagging. Thus, the process should be too fast to influence the width of the H8 signals, and the broadness observed is more likely to be due to a more signifcant dynamic motion such as that between HH and HT forms.

In addition to the *cis*-Pt(NH$_3$)$_2$(GpG) H8 signal line width, H8 signal shift dispersion and shift together provide another important indication of the probable presence of multiple variants. These H8 signals have an average value of 8.43 ppm and are not so highly dispersed (only 0.23 ppm) as the ∼1 ppm value for the typical retro-model HH variant. The average of the two H8 shifts is 8.60, 8.44, and 7.90 ppm for the **Bip**Pt-(GpG) HH1 L, HH1 R, and ΔHT1 variants, respectively. One can rationalize the small dispersion and the intermediate average shift of *cis*-Pt(NH$_3$)$_2$(GpG) if it is a mixture of HH1 R (∼65−70%), HH1 L (∼20−25%), and ΔHT1 (∼10%) conformers. Such a mixture is consistent with most of the sugar shifts, as well as the H1′ coupling constant (Table 1).

At pH 10, the N1H's of *cis*-Pt(NH$_3$)$_2$(GpG) are deprotonated; significant pH-dependent changes were observed in the NMR spectrum (Table 3). The dramatic upfield shift of the 5′-G was also noted in early reports[18,42] and was later attributed to a change from an HH1 R variant to an (N1H deprotonated) HH1 L variant (with *both* H8 signals upfield).[20] However, our evidence indicates that the N1H deprotonation cannot result only in a simple change in handedness of the HH1 conformer. The 3′-G H8 shift of ∼8.2 ppm is almost 1 ppm upfield of the ∼9.1 ppm value for an N1H-deprotonated HH1 L variant expected from our **Bip**Pt results. An increase in the population of the

HH1 L variant would result in an upfield shift of the 5′-G H8 signal, but it would also result in a *downfield* shift of the 3′-G H8 signal (Table 3). The observed *slight* upfield shift of the 3′-G H8 signal of *cis*-Pt(NH_3)$_2$(GpG) suggests an increase in the population of several variants; such an increase would have a canceling effect on the shift of the 3′-G H8 signal, explaining the insensitivity of its shift to pH. Because the NH_3 groups would project H's to either side of the coordination plane and for both positions cis to the G residues, high pH can favor both ΔHT1 and ΛHT2 variants since two strong G O6-**Bip** NH bonds could form at high pH. Such HT forms could be present in the mix of *cis*-Pt(NH_3)$_2$(GpG) forms at high pH. We have also rationalized H8 line widths of *cis*-Pt(NH_3)$_2$(GpG) using this type of reasoning (Supporting Information).

Finally, a molecular dynamics study of *cis*-Pt(NH_3)$_2$(GpG)[47] in its normal protonated state suggested that a water-mediated hydrogen bond between the 5′-G 2′-OH and the phosphate group, which was possible for the anti,anti HH1 R variant but not the L variant, stabilized the R variant for *cis*-Pt(NH_3)$_2$(GpG). Although our models suggest a direct rather than water-mediated 5′-G 2′-OH-phosphate group hydrogen bond, our calculations support the previous conclusion that hydrogen bonding involving 5′-G 2′-OH stabilizes the HH1 R variant relative to the L variant. Furthermore, although the R variant is not completely dominant, it appears to be the most abundant form. In addition, our data indicate no difference in the relative stability of L variants between GpG and d(GpG) adducts, in further support of the early calculations suggesting the importance of H-bonding. Our results indicate that the observed corresponding **Bip**Pt variants for the GpG and the d(GpG) adducts have dinucleoside monophosphate moieties with very similar structures. One can reasonably believe that the spectral differences between the dynamic *cis*-Pt(NH_3)$_2$ GpG and d(GpG) adducts arise from the effect of this H-bonding on the relative stability of the variants and that the corresponding variants have the same general structure.

Conclusions

No HH2 variant was found for the **Bip**Pt(GpG) adducts; the absence of any variant of the unusual HH2 form is the main difference found between the **Bip**Pt GpG and the d(GpG) adducts. The three dominant **Bip**Pt(GpG) variants that were found here at low pH have very similar spectral features, including the newly obtained CD signals, as the three corresponding **Bip**Pt(d(GpG)) variants. Thus, the observed GpG and d(GpG) variants are structurally very similar. The three dominant **Bip**Pt(GpG) forms are the first distinct N7−Pt−N7 GpG variants with separately characterizable NMR features. (In previous studies,[24,25] a mixture of two forms was observed, but our data suggest each is likely to be a mixture of rapidly interconverting variants.) The hydrogen bond between the 5′-G 2′-OH and the phosphate group, which was possible for the anti,anti HH1 R variant but not for the L variant of GpG adducts, appears to stabilize the (*R*,*S*,*S*,*R*)-**Bip**Pt(GpG) R variant at the expense of the anti,anti HH2 R variant. (*S*,*R*,*R*,*S*)-**Bip**Pt(GpG) is a mixture of anti,anti HH1 L and anti,syn ΔHT1 L variants. The equilibrium ratio of these variants is nearly exactly the same as that found for (*S*,*R*,*R*,*S*)-**Bip**Pt(d(GpG)), a result supporting the absence of an H-bonding effect for the 2′-OH group in the L variant.

Studies with other carrier ligands are needed to achieve a complete understanding of the effects of the 2′-OH group. Such studies may also eventually reveal any influence that the carrier ligand may have on the spectral properties. However, at this time, distinct spectral patterns are emerging for the various variants we have identified. Analysis of the NMR shifts and CD signal shapes indicates that *cis*-Pt(NH_3)$_2$(GpG) exists mostly as the HH1 R conformer, as suggested previously in the literature.[20] However, at low pH other conformers account for perhaps one-third of the complex.

At high pH, the conformer distribution changes. Although it appears to be reasonable that the HH1 L variant is now a more abundant form, it is not the exclusive form. Other forms likely to be present include the ΔHT1 form, which accounts for the upfield shifts with pH of the ^{31}P NMR signal. However, at this time it appears likely that other forms may be part of the *cis*-Pt(NH_3)$_2$(GpG) mix at high pH. One of the possibilities is a *cis*-Pt(NH_3)$_2$(GpG) ΛHT2 form; such a form appears to be a minor component at high pH for (*R*,*S*,*S*,*R*)-**Bip**Pt(GpG), although it is absent at low pH. Because of the additional complexity associated with the possibility of stronger G O6 H-bonding to the carrier ligand, additional studies are needed before the high-pH conditions can be understood. However, our results leave little doubt that non-HH1 forms are present for *cis*-Pt(NH_3)$_2$-(GpG) at both high and low pH.

Acknowledgment. This work was supported by NIH Grant GM 29222 (to L.G.M.), NATO CRG 950376 (to L.G.M. and G.N.), and MURST (Contribution ex. 40%), CNR, and EC (COST Chemistry project D8/0012/97) (to G.N.). We thank Dr. Susan Ano for performing preliminary work on this project.

Supporting Information Available: Descriptions of the ^{1}H NMR signal assignments; tables of the ^{1}H NMR chemical shifts of *cis*-Pt(NH_3)$_2$(GpG) at low and high pH; solvent-exposed areas of hydrogen-bonded atoms from unrestrained calculations of (*R*,*S*,*S*,*R*)-**Bip**Pt(GpG); and figures of partial 2D NMR spectra of (*S*,*R*,*R*,*S*)-**Bip**Pt(GpG) and *cis*-Pt(NH_3)$_2$(GpG), stereoviews of energy-minimized structures of HH1 R and HH2 R conformers of (*R*,*S*,*S*,*R*)-**Bip**Pt(GpG), enlarged CD spectra of *cis*-Pt(NH_3)$_2$(GpG) superimposed with **Bip**Pt(GpG) spectra, partial ^{1}H NMR spectra of *cis*-Pt(NH_3)$_2$(GpG) at low and high pH, exchange pathways for *cis*-Pt(NH_3)$_2$(GpG) (PDF), and the coordinates of calculated structures of the three observed variants of **Bip**Pt(GpG) (PDB). This material is available free of charge via the Internet at http://pubs.acs.org.

JA994305T

(47) Kozelka, J. In *Platinum and Other Metal Coordination Compounds in Cancer Chemotherapy*; Pinedo, H. M., J. H. Schornagel, Eds.; Plenum Press: New York, 1996; pp 37−42.

(48) Kline, T. P.; Marzilli, L. G.; Live, D.; Zon, G. *J. Am. Chem. Soc.* **1989**, *111*, 7057−7068.